Kappa but not delta or mu opioid receptors form homodimers at low membrane densities

Kristina Cechova[1,2], Chenyang Lan[3], Nicolas P. F. Barthes[4], Manfred Jung[4,5], Maximilian H. Ulbrich[6,7,*]

[1]Department of Biomathematics, Institute of Physiology, Academy of Science of the Czech Republic

[2]Department of Biochemistry, Faculty of Science, Charles University

[3]Faculty of Biology, University of Freiburg

[4]Institute of Pharmaceutical Sciences, University of Freiburg

[5]CIBSS – Centre for Integrative Biological Signalling Studies, University of Freiburg

[6]Institute of Internal Medicine IV, Medical Center of the University of Freiburg

[7]BIOSS Centre for Biological Signalling Studies, University of Freiburg

*corresponding author

Abstract

Opioid receptors (ORs) have been observed as homo- and heterodimers, but it is unclear if the dimers are stable under physiological conditions. Here we use three live-cell imaging approaches to assess dimerization of ORs at different expression levels. At high membrane densities, a split GFP assay reveals that κOR dimerizes, while μOR and δOR stay monomeric. In contrast, single-molecule imaging showed no κOR dimers at low receptor densities. To reconcile our seemingly contradictory results, we used a high-density single-molecule assay to assess membrane protein interactions at densities 100x higher than conventional single-molecule imaging. We observe that κOR is monomeric at low densities and forms dimers at densities that are considered physiological. In contrast, μOR and δOR stay monomeric even at the highest densities covered. The observation of long-lasting κOR dimers but not higher order aggregates suggests that OR dimerization is a specific effect and not a result of increasing expression.

Introduction

ORs are G protein-coupled receptors (GPCRs) from class A with three genes coding for the δOR, κOR, and μOR. Based on pharmacological profiles, more subtypes were proposed, which can be explained by the existence of splicing variants, posttranslational modifications and/or direct interactions between receptors. Dimerization of ORs has been covered in multiple studies, yet the conclusions were contradictory, as for many other GPCRs, likely due to the use of differing methodological approaches and experimental conditions [1].

So far, the major techniques to assess dimerization of ORs were co-immunoprecipitation followed by Western blotting, and bioluminescence resonance energy transfer (BRET) [2–6]. Both are bulk techniques, where the signal is obtained from a large population of cells. Not only is the major part of the signal caused by a small, highly expressing fraction of the cells, but in addition, these few cells express the receptors at the highest density. Therefore, the signal mainly reflects the receptor's behavior at a membrane density that is far above the physiological range, but cannot capture the state of the receptors at low membrane densities, as they prevail in many cells *in vivo*.

In this work, we quantitatively measured OR dimerization using different microscopy approaches that work at different densities. Our starting point was a split GFP fluorescence complementation assay in cells with expression levels of 50–100 / µm^2. This assay gave us a first indication that the κOR has a tendency to dimerize, while the δOR and μOR resembled the monomeric control, which was the PDGFRα transmembrane domain (PDGFRTM). However, with conventional dual-color single-molecule imaging at densities below 5 / µm^2, we did not observe a significantly higher dimerization for κOR than for the other ORs. Therefore, we turned to a recently developed technique called PhotoGate that allows tracking of single molecules in an originally crowded environment by controlling the density of fluorescent molecules in a region of interest [7]. We quantified the monomer/dimer ratio at densities of up to 200 / µm^2, a level that is thought to be in the physiological range for many GPCRs. δOR and μOR remained predominantly monomeric at all densities tested, whereas κOR formed dimers at higher levels, with a dissociation constant of k_d = 15±8 / µm^2.

Results

Single-molecule split GFP complementation suggests higher dimer fraction for κOR

To assess dimerization of ORs, we used a three-color single-molecule approach for determining absolute densities of membrane proteins in combination with fluorescence complementation of a split GFP. The complementation of non-functional GFP fragments to recover fluorescence upon their encounter has previously been used with different split positions. Here, we used the split position between the 10th and 11th beta strand of the GFP barrel, yielding one fragment containing the first ten strands (GFP10), and one fragment containing the last strand (GFP11) [8]. The two constructs carrying GFP10 and GFP11 were additionally tagged with mKate, which emits in the orange range, and the SNAP-tag, which we labeled with a far-red substrate. By comparing the intensities emitted from highly expressing cells with intensities of single molecules of GFP, mKate and the far-red labeled SNAP-tag, we calculated the absolute densities of these species in the membrane.

We generated pairs of δOR, κOR, or μOR, or the PDGFRTM as a negative control, fused with an N-terminal SNAP-tag and C-terminal GFP10, or C-terminal GFP11 and mKate, respectively, resulting in SNAP-X-GFP10 and X-GFP11-mKate, where X was δOR, κOR, or μOR, or PDGFRTM (Fig. 1a). CHO cells expressing a matching pair were labeled with the far-red fluorescent dye Alexa Fluor 647 conjugated to benzylguanine (BG647), and consecutively imaged with 488 nm, 561 nm, and 637 nm excitation in Total Internal Reflection (TIR) configuration (Fig. 1b). After taking a snapshot in each wavelength range, we photobleached nearly all fluorophores and recorded short movies where only a few unbleached molecules were sparsely distributed and showed clear photobleaching steps (to confirm that they were from single molecules) (Fig. 1c).

From the background-subtracted intensities of single molecules and the initial snapshots of the unbleached cell membrane, we determined the surface densities of reconstituted GFP, mKate, and BG647-labeled SNAP-tag (SNAP647) molecules. We selected cells with a similar density of mKate and SNAP647, and calculated the GFP-positive fraction as the ratio of GFP density to the smaller value of mKate and SNAP647 densities (since the smaller one is limiting the number of molecules available for dimerization). For PDGFRTM, the GFP-positive fraction was 53 ± 9% (s.d., n = 8), and the smaller one of the mKate and SNAP647 surface density 23 ± 18 / μm², for δOR 48 ± 21% (26 ± 23 / μm^2, n = 10), for κOR 91 ± 11% (26 ± 22 / μm^2, n = 9), and for the μOR 33 ± 11% (23 ± 15 / μm^2, n = 7) (Fig. 1d).

The larger GFP-positive fraction for the κOR than for the negative control PDGFRTM, δOR, and μOR suggests that the κOR has a higher tendency to dimerize that the other two ORs. The PDGFRTM, which served as a negative control since it is thought to be monomeric, also had a surprisingly high GFP-positive fraction. An explanation could be that spontaneous encounters of proteins in the cell membrane bring the GFP fragments sufficiently close to each other to lead to a reconstitution of the GFP fluorescence. Since GFP10 and GFP11 do not separate again once they are connected, the GFP-positive fraction increases to a much higher value than what would be expected from interaction of the untagged target proteins. The GFP-positive fraction for δOR and μOR is similar to PDGFRTM, which gave us a first indication that they might be monomeric as well.

Single-molecule imaging does not show more dimers for κOR than for δOR and μOR

The split GFP approach indicated an increased dimer fraction for κOR, but an accurate quantification using this approach is impossible due to the stickiness of the GFP fragments. Also, the efficiency of GFP fluorescence recovery upon complementation is unknown, and therefore, the split GFP approach can only deliver a qualitative description. For these reasons, we chose a more direct approach and imaged differentially labeled receptors in the cell membrane on a single-molecule level. When the single receptor molecules are separated in the average by a distance that is large compared to the diffraction limit of ~ 200 nm, then co-localization of the fluorescent spots amounts to dimerization. Accordingly to minimize co-localization caused by random encounters, the density in the membrane has to be kept sufficiently low. Since we abstained from the use of the split GFP and also introduced the mutation A206K that virtually eliminates the tendency of GFP to dimerize, the dimer fraction of the ORs should not be affected by interactions of the tags [9].

We fused a C-terminal monomeric GFP or an N-terminal SNAP-tag to the target proteins, hereby obtaining X-GFP and SNAP-X, where X was δOR, κOR, μOR, or PDGFRTM. The SNAP-tag was labeled with a conjugate of the orange-red dye DY549-P1 and benzylguanine (SNAP549) (Fig. 2a). We recorded 488 nm / 561 nm excitation dual-color movies of CHO cells expressing one of the X-GFP/SNAP549-X pairs (Fig. 2b and Suppl. Movie 1). We imaged cells with low surface densities of < 5/μm^2 of the proteins because with higher expression, individual molecules could not be separated from each other and random co-localization of the green and red emission from GFP and SNAP549 became too high. For all four protein pairs, we observed red and green fluorescent spots, and in a minor fraction of spots, red and green signals overlapped.

To assess the overlap, we selected a representative area of the cell and manually determined the number and positions of the spots in the green and red channels (Fig. 2b). Spots where the position in the two channels differed by 250nm or less were classified as overlapping and referred to as 'yellow' in the following. The average fraction of monomers in yellow spots was 19 ± 11% (s.d., n = 16 cells) for δOR, 22 ± 9% for κOR (n = 17), 20 ± 8% (n = 15) for μOR and 23 ± 8% (n = 7) for the negative control PDGFRTM (Fig. 2c). We also evaluated the time that green and red spots remained co-localized in consecutive frames of the movies. For δOR, we obtained 143 ± 85 ms (s.d., n = 51 spots), for κOR 163 ± 97 ms (n = 42), for μOR 190 ± 123 ms (n = 42), and for PDGFRTM 130 ± 74 ms (n = 41) (Fig. 2d). Although the time for co-localization was low for all four protein pairs, we rarely but repeatedly observed yellow spots in the κOR experiment where green and red co-localized and diffused together (Fig. 2e and Suppl. Movie 2, 3). However, they occurred only at a frequency that was not statistically significant.

In the single-molecule tracking and co-localization, we did not observe a larger fraction of yellow spots, or a longer time of co-localization for the κOR than for the δOR, μOR, or the negative control PDGFRTM, in contrast to what we expected from the higher GFP-positive fraction in the split GFP assay. It is possible that under the low expression conditions used here, there is no significant level of dimerization for any of the proteins studied, and that the observed overlap is due to random co-localization without direct interaction. An alternative explanation for the sizeable degree of co-localization is that all proteins, including the presumably non-dimerizing PDGFRTM, have a small tendency to dimerize.

Single-molecule imaging of highly expressing cells with PhotoGate reveals κOR dimers

How can we resolve the apparent discrepancy between the results we obtained from the split GFP experiments, where κOR had a higher GFP-positive fraction than δOR and μOR, and the single-molecule imaging, where κOR had a similar fraction of yellow spots as the other two ORs and the (presumably monomeric) control? One explanation that would reconcile these findings is that the dissociation constant for κOR is above the density from the single-molecule experiments, but below the density in the split GFP assay. Then, as we would expect for non-covalent binding, monomers and dimers can interconvert and a higher density should shift the equilibrium to a higher dimer fraction.

To experimentally support this idea, we want to use a single-molecule co-localization approach that works at higher densities of molecules in the membrane. Two techniques called TOCCSL (Thinning Out Clusters while Conserving the Stoichiometry of Labeling) and PhotoGate were previously designed for this purpose [7,10] (Fig. 3a). In a highly expressing cell, a part of the cell membrane gets photobleached quickly. After a recovery time, unbleached molecules re-populate the bleached area by lateral diffusion. The resulting density in the bleached area will be lower than the initial density. If the time allowed for recovery is shorter than the time for protein complexes to dissociate, the intact complexes can be imaged at lower density. In the PhotoGate technique, in addition to the initial bleaching exposure, a thin ring of high intensity is projected at certain time intervals to keep the density in the central imaging area low. In order to reduce glare from the highly expressing part of the cell, an iris is used to restrict the illumination used for imaging to the low expressing area.

We used the same constructs as for the previous experiment, i.e. we co-expressed X-GFP and SNAP549-X, where X was δOR, κOR, μOR or PDGFRTM. However, this time we selected cells expressing a high density of molecules. In a small circular area of the cell with 10–15 µm diameter, GFP and SNAP549 were completely bleached with a focused laser beam. Then the laser was off for 5–20 s, depending on the expression level of the cell, to let molecules diffuse into the bleached area. Several rings were drawn at the outer edge of the bleached area to control the amount of recovery while allowing molecules inside the ring to distribute evenly. Finally, a two-color movie of the central area was recorded (Fig. 3b, c). Eventually, the remainder of the cell was imaged to determine the intensity per area and, by comparison to the unitary intensity of a single molecule, to calculate the density of molecules in the cell membrane.

Again, the overlap was assessed by selecting green and red spots and classifying as yellow the spots where center positions were apart 250nm or less. The average fraction of receptors in yellow spots and co-localization times were 16 ± 6% (s.d., n = 15) and 155 ± 117 ms (n = 79) for δOR (avg. density in the unbleached cell 64 ± 40 / µm^2), 33 ± 10% and 476 ± 449 ms for κOR (n = 15/78, 55 ± 35 / µm^2), 17 ± 6% and 120 ± 75 ms (n = 15/62, 43 ± 32 / µm^2) for μOR and 15 ± 7% and 124 ± 66 ms (n = 14/72, 64 ± 37 / µm^2) for PDGFRTM (Fig. 3d, e and Suppl. Movies 4–7). At the high membrane densities, the κOR shows a much higher co-localization of green and red than δOR, μOR or the PDGFRTM control. This supports our assumption that an increased density shifts the equilibrium from monomers to dimers for κOR. Since PDGFRTM, δOR and μOR have no tendency to dimerize, they stay monomeric.

Dissociation constant of κOR

Finally, we set out to estimate the dissociation constant by analysis of the density dependence of the co-localization. We plotted all values of the yellow fraction obtained from the PhotoGate experiments as a function of total spot density including green, red and yellow (Fig. 4a). We observe that for δOR, μOR and PDGFRTM, there is no trend for a higher yellow fraction at higher densities. However, for κOR, the yellow fraction increases from a low value of 10% at a density of 14 / μm^2 to a high value of 46% for densities of > 100 / μm^2, with a shape reminiscent of a binding curve, again giving support to the notion that the κOR dimer fraction increases with density. Importantly, the fraction of yellow spots converged towards a limiting value for increasing densities, suggesting that no higher order clusters were formed; in this case, we would have expected the fraction of yellow spots to further increase and reach levels above above 50%, because in higher order clusters, the chances are high to have both green and red labeled receptors.

In principle, we would expect the dimer fraction to increase from 0% to nearly 100%. In fact, the value we measured was not the dimer fraction, but the fraction of yellow spots, which is not the same. First, as noted above, yellow spots can also appear due to random co-localization without direct interaction. But the major factor that causes the fraction of yellow spots to be limited are the dimers formed from two green or two red spots, and dimers including a non-fluorescent GFP or unlabeled SNAP-tag, which all will result in dimers appearing as only green or only red spots. To correct for the different effects, we established a model that accounts for random co-localization, monomer and dimer fractions, non-fluorescent GFP and unlabeled SNAP-tag, and the green/green and red/red dimers (Fig. 4b and Suppl. Note 1). We measured the fraction of non-fluorescent GFP and the fraction of unlabeled SNAP-tag in an experiment with SNAP549-PDGFRTM-GFP. Since every molecule carries both tags, the non-fluorescent/unlabeled fractions can directly be determined from the fraction of green, red, and yellow spots (Suppl. Note 2). The fraction of non-fluorescent GFP was 53 ± 3%, the fraction of unlabeled SNAP-tag was 62 ± 2% (n = 14, s.e.m.).

The model allowed us to calculate the fraction of receptors in dimers from the fraction of yellow spots. In the case of dimerization, the resulting curve can be described by the equation

$$f_d = 1 + \left(k_d - \sqrt{k_d(k_d + 8[R])}\right)/4[R]$$

with the dissociation constant k_d and the receptor density $[R]$, corrected for non-fluorescent GFP and unlabeled SNAP-tag (Suppl. Note 3). For the κOR, a nonlinear fit yielded the dissociation constant k_d = 15±8 / μm^2 (Fig. 4c). For the δOR and μOR, the dimer fractions were in the range of the monomeric control PDGFRTM for all receptor densities. Taken together, we conclude that κOR forms dimers at expression levels above 20 / μm^2, but δOR and μOR stay monomeric, at least at densities up to 200 / μm^2.

Discussion

In this study we used a split GFP complementation assay, conventional single-molecule imaging and the PhotoGate single-molecule technique to assess the dimerization of ORs. We find that κOR forms homodimers at densities below 200 / μm^2, while δOR and μOR stay monomeric. The dissociation constant for κOR is k_d = 15±8 / μm^2. We observe that co-localization of green and

red labeled receptors of the δOR, the μOR and the monomeric control is only transient, whereas κOR forms long-lasting dimers at the same densities. Moreover, the lack of higher-order aggregates for high receptor densities suggests that the dimerization is a specific effect and not caused by coincidental co-localization or clustering at cellular structures.

In general, it is difficult to measure lateral affinities of membrane proteins because of the inability of biochemical methods to determine the density of the target protein in the plasma membrane. So far, this can only be achieved with fluorescence based assays where the signal from the labeled protein in the membrane of a living cell can be compared to a reference of known concentration or a direct observation of single molecules is possible. With conventional single-molecule imaging, maximum densities of 5 / μm^2 are accessible [11,12]. With bulk fluorescence methods using confocal microscopy, the minimum measured densities were 160 / μm^2 [13–15]. The PhotoGate approach we used covers the missing range of 10–100 / μm^2. It remains to be seen if measurements from the three ranges can be consolidated into a common framework.

A major contribution to the error in the dissociation constant originates – as for many single-molecule methods – from the uncertainty inherent to counting low numbers of events, in our case the green, red and yellow spots. The uncertainty in the initial counts (Fig. 4a) gets even amplified when subtracting the expected number of yellow spots caused by random co-localization (Fig. 4c). A second error source that is difficult to account for is the variability of the SNAP-tag labeling efficiency. In the model to calculate the fraction of dimers from the fraction of yellow spots, we used the average SNAP-tag labeling efficiency, but the actual labeling efficiency might vary from one cell to another, e.g. due to different accessibility of the substrate in the extracellular solution to the cell.

A possible source for a systematic error that is more difficult to compensate lies in the design of the PhotoGate technique. A delay is required between the initial bleaching and the movie acquisition to allow molecules from the outside to diffuse into the bleached center (Fig. 3a). In our experiments, this delay was in the range of 20 s. If receptor dimers dissociate in a comparable time frame, then a significant fraction of the dimers will have decayed by the time of imaging, and will therefore appear as monomers. However, we estimate that this effect reduces the dimer fraction by less than 10% in the case of the κOR since we obtained a large dimer fraction for high membrane densities. In principle, it is possible that the δOR and/or μOR dimer fractions are affected by this fast dissociation into monomers, and that our interpretation of δOR and μOR to be monomers at all tested densities is incorrect. However, one would then expect the GFP positive fraction in the split GFP assay to be larger than what we observed. Therefore we think that our experiments are consistent with δOR and μOR being monomers at the densities we observed.

Whether the ORs form homo- and heterodimers is strongly debated. From co-immunoprecipitation, BRET experiments, and functional studies, both homo- and heterodimers for all combinations of δOR, κOR, and μOR have been observed [2–6,16,17]. Some studies claimed that no dimers are visible, and in one case, a dependence of dimer formation on G protein binding has been postulated [18,19]. For many studies, the receptors were expressed under control of the strong CMV promoter; in our work, we used a promoter with inducible expression and selected cells with receptor densities of 200 / μm^2 or less. Therefore, to understand whether the different expression levels could be a possible cause for the apparent discrepancies, we measured the membrane densities of δOR when expressed under the CMV promoter. We found

that although a majority of cells expressed under 500 receptors/μm^2, receptor densities reached up to 6000 / μm^2 (Suppl. Fig. 1). But because the higher expressing cells contain more receptors, only a small fraction of 4% of the receptors experience densities below 500 receptors/μm^2, and more than half of the receptors reside at densities above 3000 / μm^2. Therefore, bulk experiments (e.g. BRET and co-IP) will mainly yield the signals from the high density cells. Accordingly, our observation that δOR and μOR are monomeric could be reconciled with other studies if the dissociation constants of δOR and μOR lies above 200 / μm^2.

Some current sources offer data on RNA levels in all organs, which suggest that ORs are expressed in most tissues, but at strongly differing levels [20]. However, it was not determined whether just a small fraction of cells express the receptors strongly, or most of the cells at low or moderate levels. Accordingly, expression levels and membrane densities in individual cells remain unknown. To understand the impact of dimerization *in vivo*, receptor membrane densities in different cell types in the body need to be measured in the future.

Materials and Methods

DNA constructs

The murine δ- and κ-opioid receptor, rat μ-opioid receptor, and the transmembrane domain of PDGFRα were cloned into the pWHE636 vector (gift by Christian Berens) that contains a tetracycline inducible promoter [21]. An N-terminal signal peptide and the SNAP-tag were fused to the N termini and GFP to the C-termini of the receptors and PDGFRTM with flexible linkers. In order to have well-folding, soluble domains on both sides of PDGFRTM, we added a non-fluorescent mEGFP carrying the mutation Y66I (to render it non-fluorescent) to the C-terminus of SNAP-PDGFRTM, and a signal peptide, followed by a HALO-tag, to the N-terminus of PDGFRTM-GFP. For split GFP, β-sheets 1–10 (aa 1–214) of a GFP variant were fused to the constructs with the SNAP-tag, and β-sheet 11 (aa 215–230) and mKate to the constructs without SNAP-tag [Cabantous 2005].

Expression of ORs in CHO cells

For inducible expression in mammalian cells, a stable CHO-K1 cell line (ATCC) was made with the regulator plasmid pWHE644 containing a tetracycline-regulated transactivator and a transcriptional silencer [Danke 2010]. The cells were seeded on a high refractive index coverslip (n = 1.78) and grown in complete DMEM for 12–15 h to obtain 60–80% confluency before transfection with polyethylenimine (1 mg/ml) with 1 µg of each DNA per coverslip. After 3 h, cells were washed in DPBS and incubated with doxycycline in DMEM to induce expression. The induction was terminated by washing with DPBS, and then complete DMEM was added to cells. Imaging started after 12–15 h of induction of expression. For single-molecule imaging and split-GFP assay, cells were incubated for 2 h with 1 µg/ml of doxycycline hyclate, for the PhotoGate experiment for 3 h with 2 µg/ml. For SNAP-tag labeling, cells were incubated with 2 nM benzylguanine-Alexa Fluor 647 (New England Biolabs, SNAP-Surface Alexa Fluor 647) or custom synthesized SNAP substrate benzylguanine-DY549P1 for 30 min before an experiment, and unbound dye was washed away by rinsing 5x with DPBS.

Dye synthesis

HPLC analysis (1 mL/min) and purification (3 mL/min) were performed on an Agilent Technologies 1260 Infinity system using UV detection at 290 nm and – for analysis – a Phenomenex Kinetex® 5u XB-C18 100 Å 250 x 4.6 mm column or – for purification – a Phenomenex Synergi® 10u Hydro–RP 80 Å 250 x 15.0 mm column. Eluent A was water containing 0.05 % trifluoroacetic acid (TFA) and eluent B was acetonitrile containing 0.05 % TFA. Linear gradient conditions were as follows: 0–1 min, A/B (90:10); 1−21 min, linear increase to 100 % of B; 21−23 min, 100 % B; 23–23.3 min: A/B (90:10); 23.3–26 min: A/B (90:10). Characterization was performed through mass spectrometry and mass spectra were recorded on a Thermo Scientific Exactive mass spectrometer using electrospray ionization (ESI) as ion sources.

To a stirred solution of 6-((4-(aminomethyl)benzyl)oxy)-7*H*-purin-2-amine (1.4 mg, 5.2 µmol, 1.1 eq.) in CH_3CN (250 µL), under inert atmosphere, was added the NHS ester of DY549-P1 (5 mg, 4.8 µmol, 1 eq.) in 250 µL of H_2O, followed by $NaHCO_3$ (50 µL of a 1 M solution: final concentration of c.a. 0.1 M) and the reaction was stirred protected from light for 48 h. After completion (RP-C18 TLC: H_2O/CH_3CN 3:7) the solvent was removed to give a pink oil. The crude SNAP549 was then dissolved in the minimum volume of methanol, and purified using preparative HPLC (see conditions above). The product was isolated as a pink oil (3.3 mg, 55 % yield). $C_{49}H_{57}N_8Na_3O_{15}S_4$ (1195.25 g/mol). HPLC: t_R = 6.935 min (82 % purity – 18 % of DY549-P1-OH remaining). ESI-HRMS(–): m/z calcd for $C_{49}H_{56}N_8Na_3O_{15}S_4$: 1193.2447 $[M–H]^–$; found 1193.2434 $[M–H]^–$; m/z calcd for $C_{49}H_{57}N_8Na_2O_{15}S_4$: 1171.2627 $[M–Na]^–$; found 1171.2611 $[M–Na]^–$; m/z calcd for $C_{44}H_{54}N_3Na_2O_{15}S_4$: 1038.2239 $[M–2AP–Na]^–$; found 1038.2229 $[M–2AP–Na]^–$.

Microscopy

Imaging was done on an Olympus IX71 base equipped with an Olympus 100x NA1.70 objective, a back-illuminated EMCCD camera (Andor iXon DV-897 BV), an emission filter wheel and an OptoSplit II beam splitter (Cairn). GFP, mKate/BG549, and BG647 were excited through a custom built total internal reflection illumination pathway either consecutively (split GFP assay) or in alternating excitation (single-molecule movies). Movies (256×256 pixels) were recorded at a frame rate of 17 or 33 Hz or, for alternating excitation, at a frame rate of 65 Hz. During the experiments, cells with similar expression levels in all channels were chosen. For single-molecule imaging without PhotoGate, cells with expression < 5 / μm^2 were selected. When a number n of experiments is given, it refers to the number of cells assessed.

PhotoGate

The PhotoGate assay was done similar as described in [7]. A 473 nm laser beam (25 mW before the objective) focused on the plane of the plasma membrane was directed using a galvo scanning system placed at an appropriate position in the light path. Despite 473nm being far from the excitation maximum for DY549-P1, the intensity of the laser was sufficiently high to photobleach the dye completely. A region of interest of diameter 10–15 µm was bleached for about 10 s, depositing a total energy of 2.5 mJ/μm^2, by moving the focused beam in a spiral motion. After a 5–20 s delay (depending on fluorophore density), 2–8 rings were drawn on the cell's surface at intervals of 3–5 s, to control the density inside the pre-bleached area. Right after, an iris in the illumination pathway was closed to restrict the illumination to the central area and eliminate glare from the bright area outside, and the movie acquisition was started.

Analysis of single-molecule images

The first fully illuminated frame for each color was analyzed. A rectangular region of interest was chosen that was completely covered by plasma membrane and had an even distribution of spots. The center positions of green and red spots were manually selected in a custom written software. The fraction of receptors in dimers was calculated as $f_d = 2N_y/(2N_y + N_g + N_r)$. When the centers of green and red spots were as close as 250 nm or less, both were combined to form a yellow spot. Only where claims about differences in distributions of kOR values to the others were made, these differences were significant (Fig. 1: $p<0.002$; Fig. 3C, D: $p<0.0001$).

Density evaluation

For calculating the density of fluorescent receptors in the split-GFP and the PhotoGate assay, the intensities of single molecules were compared to the intensities of a region of interest. First, a small region of interest (0.5×0.5 μm^2) around individual fluorescent molecules was selected, and background from a nearby region without a spot was subtracted. An average value was formed from 10–20 spots. Similarly, for an area with high density, background was selected from an area outside the cell.

Author Contributions

K. C. and M. U. conceived the study, designed experiments, analyzed the data and wrote the manuscript. C. L. and M. U. established the analysis of the data. N. P. F. B. and M. J. established the synthesis and synthesized the fluorescent SNAP-tag substrate.

Competing interests

The authors declare no competing interests.

Acknowledgements

This work was supported by Deutsche Forschungsgemeinschaft (DFG) grants UL 312/6-1, RTG 2202, and CRC 992, the Excellence Initiative of the German Federal and State Governments (EXC 294), and under Germany´s Excellence Strategy (EXC-2189 – Project ID: 390939984), the Grant Agency of the Czech Republic (GA17-05903S) and the Faculty of Science, Charles University in Prague (SVV260427/2020, FM/a/2017-2-072).

References

1. Milligan, G., Ward, J. W. & Marsango, S. GPCR homo-oligomerization. *Curr. Opin. Cell Biol.* **57**, 40–47 (2019).

2. Cvejic, S. & Devi, L. A. Dimerization of the delta opioid receptor: Implication for a role in receptor internalization. *J. Biol. Chem.* **272**, 26959–26964 (1997).

3. Jordan, B. A. & Devi, L. A. G-protein-coupled receptor heterodimerization modulates receptor function. *Nature* **399**, 697–700 (1999).

4. George, S. R. et al. Oligomerization of mu- and delta-opioid receptors. Generation of novel functional properties. *J. Biol. Chem.* **275**, 26128–26135 (2000).

5. Ramsay, D., Kellett, E., McVey, M., Rees, S. & Milligan, G. Homo- and hetero-oligomeric interactions between G-protein-coupled receptors in living cells monitored by two variants of bioluminescence resonance energy transfer (BRET): hetero-oligomers between receptor subtypes form more efficiently than between less closely related sequences. *Biochem. J.* **365**, 429–440 (2002).

6. Wang, D., Sun, X., Bohn, L. M. & Sadée, W. Opioid receptor homo- and heterodimerization in living cells by quantitative bioluminescence resonance energy transfer. *Mol. Pharmacol.* **67**, 2173–2184 (2005).

7. Belyy, V. et al. PhotoGate microscopy to track single molecules in crowded environments. *Nat. Commun.* **8**, 13978 (2017).

8. Cabantous, S., Terwilliger, T. C. & Waldo, G. S. Protein tagging and detection with engineered self-assembling fragments of green fluorescent protein. *Nat. Biotechnol.* **23**, 102–107 (2005).

9. Zacharias, D. A., Violin, J. D., Newton, A. C. & Tsien, R. Y. Partitioning of lipid-modified monomeric GFPs into membrane microdomains of live cells. *Science* **296**, 913–916 (2002).

10. Madl, J. et al. Resting state Orai1 diffuses as homotetramer in the plasma membrane of live mammalian cells. *J. Biol. Chem.* **285**, 41135–41142 (2010).

11. Kasai, R. S. et al. Full characterization of GPCR monomer-dimer dynamic equilibrium by single molecule imaging. *J. Cell. Biol.* **192**, 463–480 (2011).

12. Calebiro, D. et al. Single-molecule analysis of fluorescently labeled G-protein-coupled receptors reveals complexes with distinct dynamics and organization. *Proc. Natl. Acad. Sci. U. S. A.* **110**, 743–748 (2013).

13. Beutel, O. et al. Two-dimensional trap for ultrasensitive quantification of transient protein interactions. *ACS Nano* **9**, 9783–9791 (2015).

14. Sarabipour, S. & Hristova, K. Mechanism of FGF receptor dimerization and activation. *Nat. Commun.* **7**, 10262 (2016).

15. Stoneman, M. R. et al. A general method to quantify ligand-driven oligomerization from fluorescence-based images. *Nat. Methods* **16**, 493–496 (2019).

16. Gomes, I. et al. Heterodimerization of mu and delta opioid receptors: A role in opiate synergy. *J. Neurosci.* **20**, RC110 (2000).

17. Yekkirala, A. S. et al. *N*-naphthoyl-beta-naltrexamine (NNTA), a highly selective and potent activator of mu/kappa-opioid heteromers. *Proc. Natl. Acad. Sci. U. S. A.* **108**, 5098–5103 (2011).

18. Law, P. Y. et al. Heterodimerization of mu- and delta-opioid receptors occurs at the cell surface only and requires receptor-G protein interactions. *J. Biol. Chem.* **280**, 11152–11164 (2005).

19. Meral, D. et al. Molecular details of dimerization kinetics reveal negligible populations of transient μ-opioid receptor homodimers at physiological concentrations. *Sci. Rep.* **8**, 7705 (2018).

20. Uhlén, M. et al. Tissue-based map of the human proteome. *Science* **347**, 1260419 (2015).

21. Danke, C. et al. Adjusting transgene expression levels in lymphocytes with a set of inducible promoters. *J Gene Med* **2**, 501–515 (2010).

Figure 1

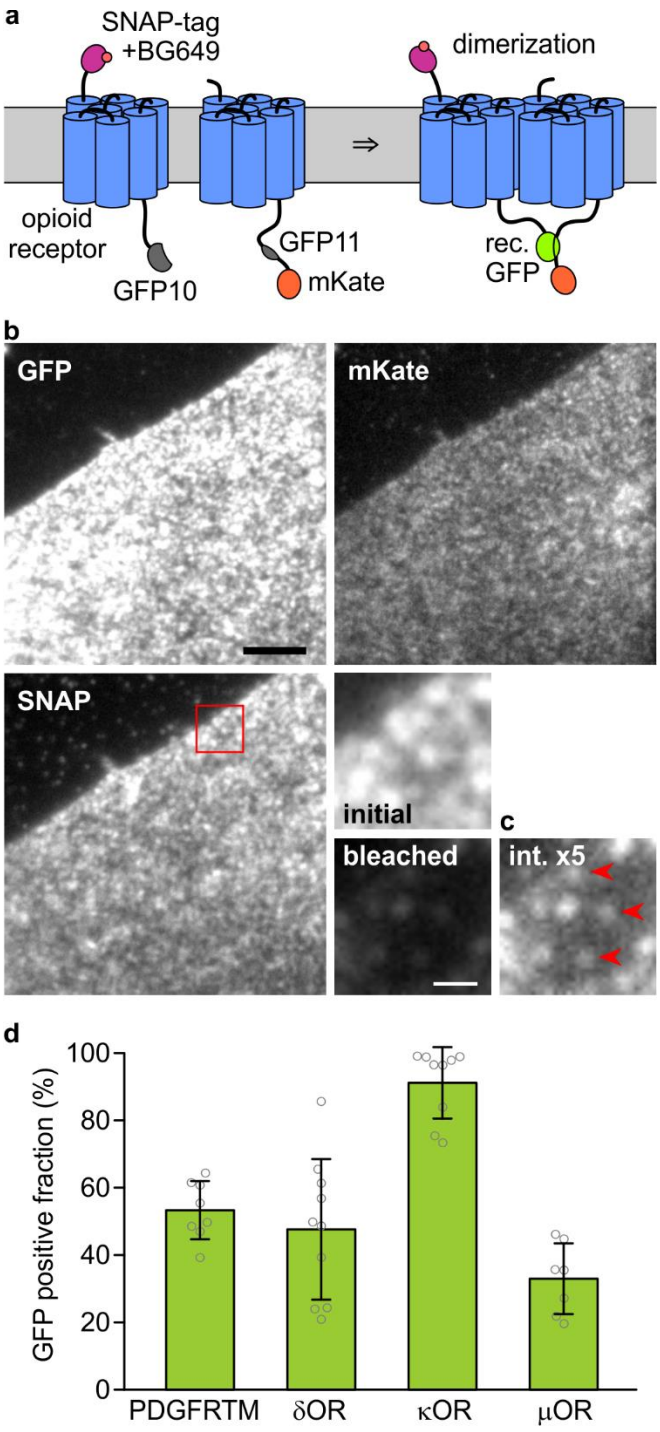

Figure 1: Split GFP assay for opioid receptor dimerization. a, To determine the densities of the two differentially labeled OR subunits, one is labeled with a SNAP-tag and its far-red fluorescent substrate BG647, and the other with mKate which emits in the orange/red range. They are also labeled with two GFP fragments. Dimerization is detected by fluorescence recovery

through complementation of the split GFP. **b**, Images of a CHO cell expressing SNAP647-κOR-GFP10 and κOR-GFP11-mKate in the three channels. The red square marks the magnified area. Scale bar 5 µm. **c**, Magnified area: Molecular densities were determined by measuring the initial fluorescence, bleaching the cell and then measuring the intensities of remaining single molecules. For the last image, the brightness is increased by a factor of 5. Red arrowheads mark single molecules. Scale bar 1 µm. **d**, The GFP positive fraction for the ORs and the monomeric control PDGFRTM was calculated from apparent densities of SNAP647, mKate, and reconstituted GFP.

Figure 2

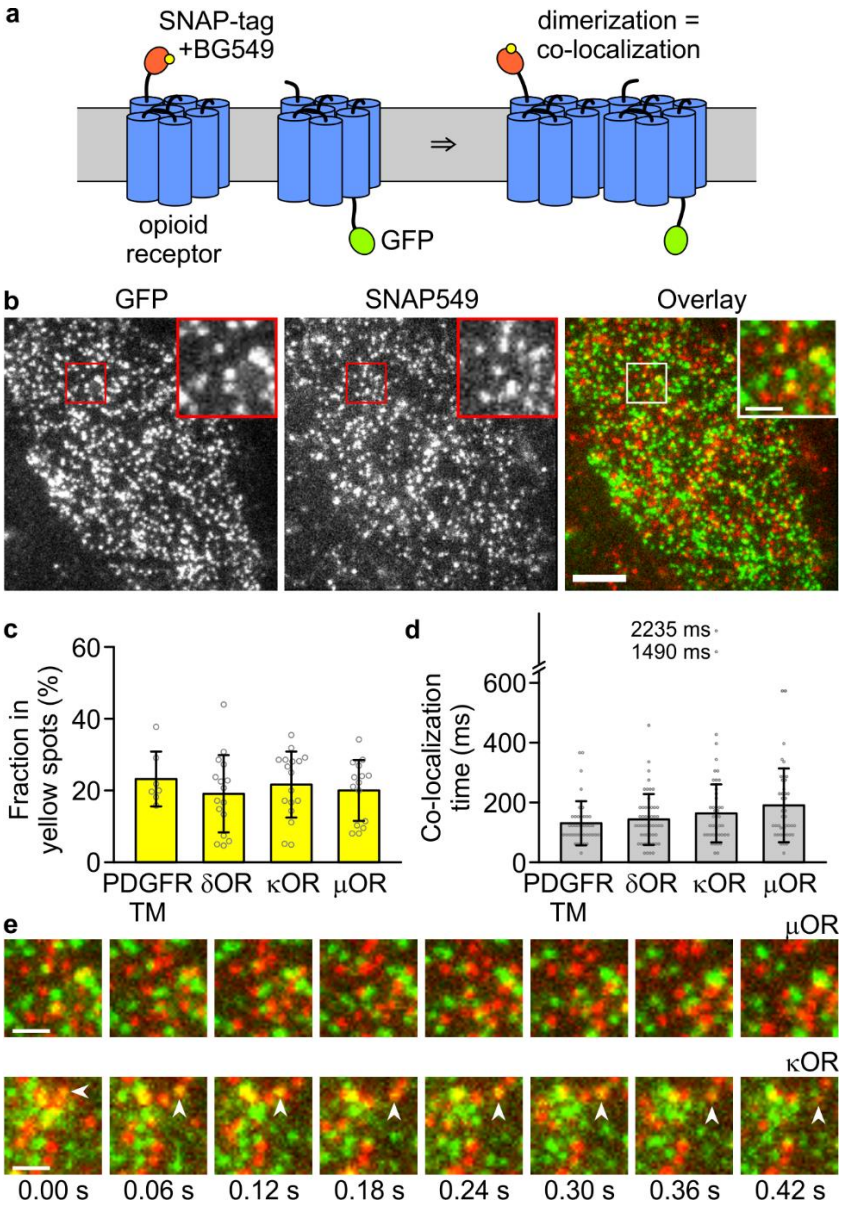

Figure 2: OR co-localization imaged on a single molecule level. a, One receptor is labeled with the SNAP-tag and BG549, the other with GFP. When the receptors, dimerize, the green and orange-red fluorescence co-localize. **b**, Still image from a dual color movie. Inset shows magnified area. Scale bar 5 µm (inset 1 µm). **c**, The fraction of spots contained in the yellow spots is similarly low for all ORs and the monomeric control. **d**, The time of co-localization of the green and red fluorescence in a yellow spot. For the κOR, rarely green and red co-localized in a yellow spot for a long time, suggesting a true interaction. Here, the two observed long-lasting co-localizations in κOR were excluded from the analysis of mean and s.d. **e**, Green and red spots that overlaid to yellow moved apart for the μOR due to diffusion. One of the long lasting co-localizing spots in the κOR (arrowhead). Scale bars 1 µm.

Figure 3

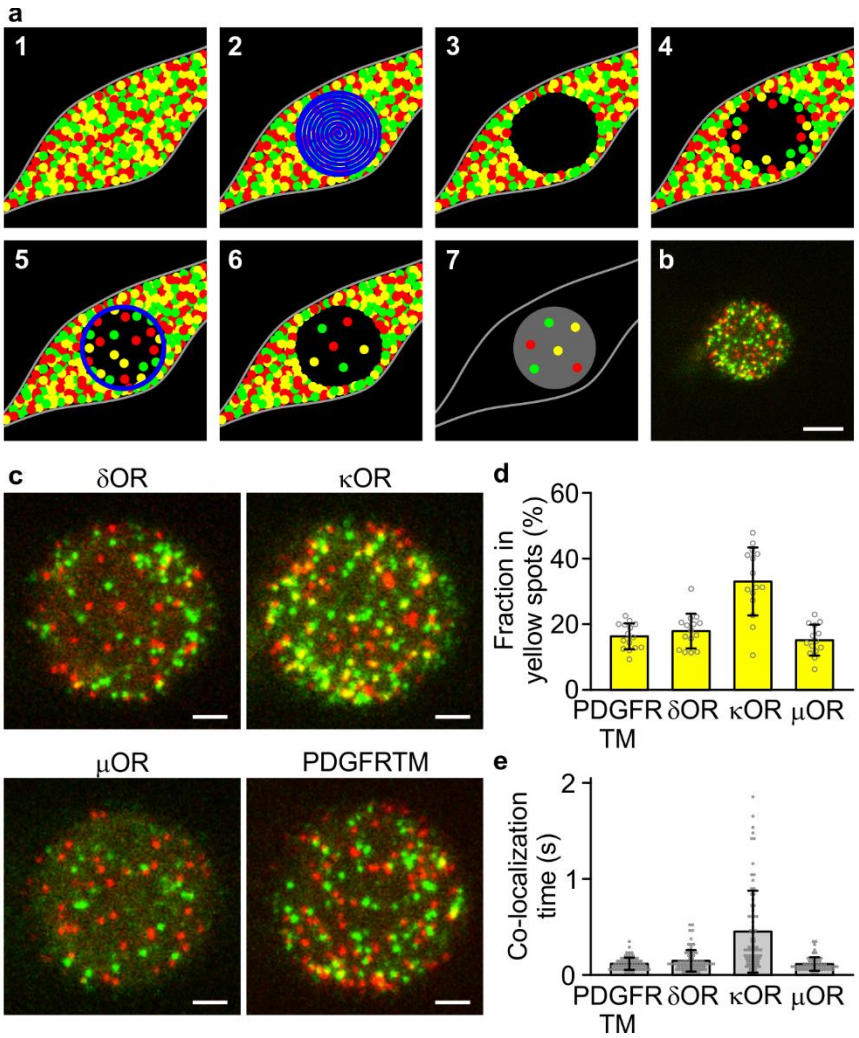

Figure 3: OR co-localization imaged with PhotoGate. a, Schematic of the PhotoGate assay [Belyy 2017]. (1) A cell with a very high membrane density of fluorescent molecules (2) gets bleached in the central part, (3) leaving a dark bleached area. (4) After a while, the bleached area gets re-populated. (5) Bleaching a ring every few seconds prevents over-population by diffusion of unbleached molecules from the edges. (6) The result is a low density in the central area. (7) For imaging, only the central part gets illuminated. **b**, First frame of a dual-color PhotoGate movie for κOR. Scale bar 5 µm. **c**, Magnified central area for the ORs and PDGFRTM. For κOR, more yellow spots are visible. Scale bars 2 µm. **d**, Fraction in yellow spots for the three ORs and the monomeric control PDGFRTM. **e**, Time of co-localization of the green and red fluorescence in a yellow spot.

Figure 4

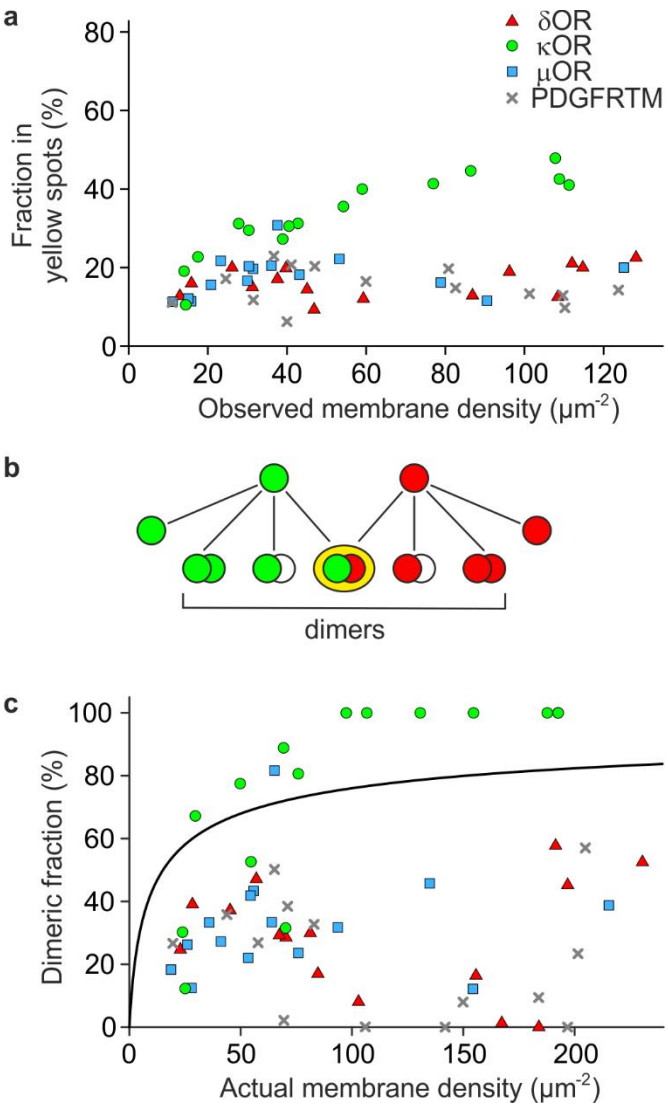

Figure 4: Dimerization of κOR. a, The fraction of molecules in the yellow spots increases with density for κOR (green circles), but stays constant for δOR (red triangles), μOR (blue squares) and the monomeric control PDGFR (grey crosses). **b**, The dimeric fraction is much larger than the fraction of molecules in yellow spots due to the non-fluorescent fraction of GFP, the unlabeled SNAP-tag, and green/green and red/red dimers. **c**, The dimeric fraction of κOR increases up to 100%, but the dimeric fractions for δOR and μOR stay in the low range of the monomeric control. A fit of a binding curve (black line) to κOR yields the dissociation constant k_d = 15±8 / μm^2.

Supplementary information

Kappa but not delta or mu opioid receptors form homodimers at low membrane densities

Kristina Cechova, Chenyang Lan, Nicolas P. F. Barthes, Manfred Jung, Maximilian H. Ulbrich

Supplementary Figure 1 2
Receptor membrane densities from expression under the CMV promoter

Supplementary Note 1 3
Model to calculate dimer fraction from yellow fraction

Supplementary Note 2 5
Model to calculate fluorescent GFP and labeled SNAP-tag fractions

Supplementary Note 3 6
Fraction of receptor subunits in dimers in dependence on total subunit density

Supplementary Movie 1
Cell expressing μOR-GFP and SNAP549-μOR (scale bar 5 µm)

Supplementary Movie 2
Cell expressing μOR-GFP and SNAP549-μOR (close-up, scale bar 1 µm)

Supplementary Movie 3
Cell expressing κOR-GFP and SNAP549-κOR (close-up, scale bar 1 µm)

Supplementary Movie 4
Cell expressing δOR-GFP and SNAP549-δOR (PhotoGate, scale bar 2 µm)

Supplementary Movie 5
Cell expressing κOR-GFP and SNAP549-κOR (PhotoGate, scale bar 2 µm)

Supplementary Movie 6
Cell expressing μOR-GFP and SNAP549-μOR (PhotoGate, scale bar 2 µm)

Supplementary Movie 7
Cell expressing PDGFRTM-GFP and SNAP549-PDGFRTM (PhotoGate, scale bar 2 µm)

Supplementary Figure 1

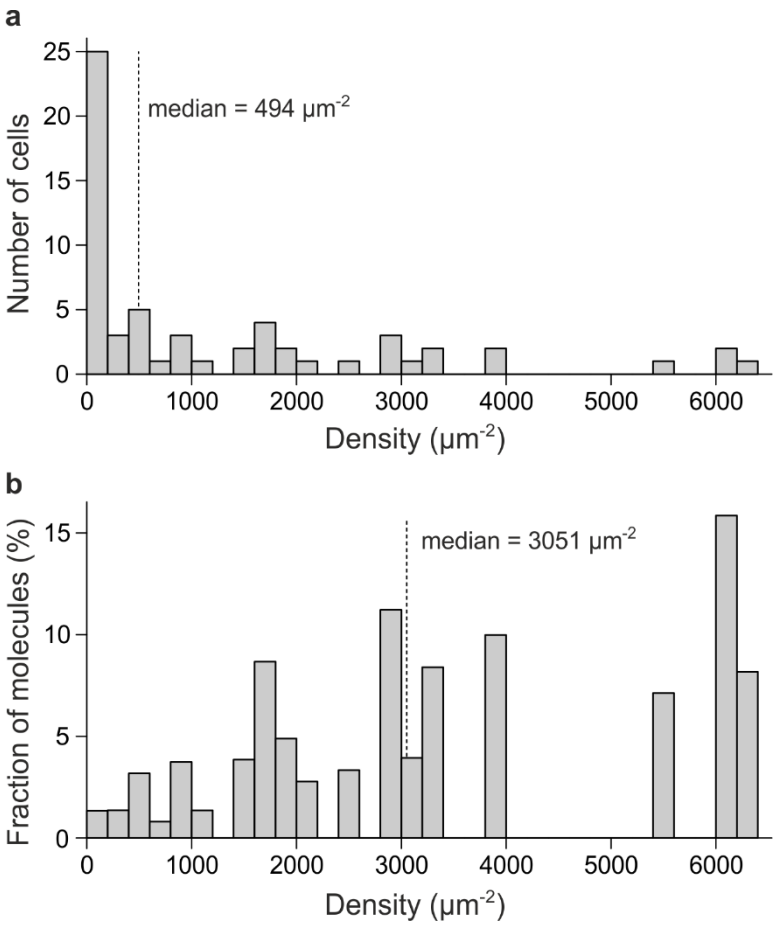

Supplementary Figure 1: Receptor membrane densities from expression under the CMV promoter. a, Histogram of δOR-GFP receptor densities at the plasma membrane taken from 60 cells. 50% of the cells express at densities below 500 receptors/μm^2, and only 15% of the cells express at 3000 receptors/μm^2 or more. **b**, A histogram of all receptors expressed at different densities, from the same cells as in (**a**). Only 4% of the receptors are at membrane densities below 500 receptors/μm^2, and 53% of the receptors reside at 3000 receptors/μm^2 or more.

Supplementary Note 1

Model to calculate dimer fraction from yellow fraction

The model takes into account the coincidental overlap of green and red florescent receptors, the formation of dimers from two green- or two red-labeled subunits, and the fractions of unlabeled SNAP-tag and non-fluorescent GFP. By assuming values for the total number of receptor subunits N_0, the fraction of total receptor subunits in monomers f_m, the fraction of GFP-labeled receptor subunits f_G, together with the known fractions of fluorescent GFP p_g and labeled SNAP-tags p_r, and the ratio of spot area A_s (spot radius r_{spot}) to area A_0 that all spots cover (i.e. the evaluated area of the membrane), we established a formula to estimate the values N_{g-spot}, N_{r-spot}, and N_{y-spot} for the observed numbers of green, red and yellow spots.

The numbers of GFP- and SNAP-labeled monomers N_{mG} and N_{mS}, and dimers carrying two GFP, two SNAP, or one of each N_{dGG}, N_{dSS}, N_{dGS} are:

$$N_{mG} = N_0 \cdot f_G \cdot f_m$$

$$N_{mS} = N_0 \cdot (1 - f_G) \cdot f_m$$

$$N_{dGG} = \tfrac{1}{2} \cdot N_0 \cdot {f_G}^2 \cdot (1 - f_m)$$

$$N_{dSS} = \tfrac{1}{2} \cdot N_0 \cdot 2 \cdot f_G \cdot (1 - f_G) \cdot (1 - f_m)$$

$$N_{dGS} = \tfrac{1}{2} \cdot N_0 \cdot (1 - f_G)^2 \cdot (1 - f_m)$$

Due to non-fluorescent GFP and unlabeled SNAP-tags, some of these can appear dark, and dimers with GFP and SNAP can appear as yellow, green, red, or dark:

$$N_{mG\to g} = N_{mG} \cdot p_g$$

$$N_{mG\to d} = N_{mG} \cdot \left(1 - p_g\right)$$

$$N_{mS\to r} = N_{mS} \cdot p_r$$

$$N_{mS\to d} = N_{mS} \cdot (1 - p_r)$$

$$N_{dGG\to g} = N_{dGG} \cdot \left({p_g}^2 + 2 \cdot p_g \cdot \left(1 - p_g\right)\right)$$

$$N_{dGG\to d} = N_{dGG} \cdot \left(1 - p_g\right)^2$$

$$N_{dSS\to r} = N_{dSS} \cdot \left({p_r}^2 + 2 \cdot p_r \cdot (1 - p_r)\right)$$

$$N_{dSS\to d} = N_{dSS} \cdot (1 - p_r)^2$$

$$N_{dGS\to y} = N_{dGS} \cdot p_g \cdot p_r$$

$$N_{dGS\to g} = N_{dGS} \cdot p_g \cdot (1 - p_r)$$

$$N_{dGS\to r} = N_{dGS} \cdot \left(1 - p_g\right) \cdot p_r$$

$$N_{dGS\to d} = N_{dGS} \cdot \left(1 - p_g\right) \cdot (1 - p_r)$$

The numbers of yellow, green, red and dark appearing receptors are the sums:

$$N_y = N_{dGS\to y}$$

$$N_g = N_{mG\to g} + N_{dGG\to g} + N_{dGS\to g}$$

$$N_r = N_{mS\to r} + N_{dSS\to r} + N_{dGS\to r}$$

$$N_d = N_{mG\to d} + N_{mS\to d} + N_{dGG\to d} + N_{dSS\to d} + N_{dGS\to d}$$

Finally, we make an approximation to correct for the random co-localization due to close vicinity of red and green receptors. Then their emission overlaps spatially, resulting in appearance of yellow spots. A green receptor will appear as yellow spot when it happens to lie within the 250 nm radius of a red receptor. Therefore, the number of green and red spots is smaller than the number of receptors labeled in these colors, and the number of yellow spots is bigger. The chance for a single green receptor to not lie on a particular red receptor is $1 - A_s/A_0$, where $A_s = \pi \cdot {r_{spot}}^2$ is the area of the spot and A_0 is the total area the counted spots cover. The chance for a green receptor to lie on any of the red receptors is then:

$$p_{rand} = 1 - (1 - A_s/A_0)^{N_r}$$

Therefore, the number of yellow spots appearing from green and red overlap is:

$$N_{y-rand} = N_g \cdot (1 - (1 - A_s/A_0)^{N_r})$$

And the final counts of green, red and yellow spots are:

$$N_{g-spot} = N_g - N_{y-rand}$$

$$N_{r-spot} = N_r - N_{y-rand}$$

$$N_{y-spot} = N_y + N_{y-rand}$$

Estimates for the total number of receptor subunits N_0, the fraction of total receptor subunits in monomers f_m, and the fraction of GFP-labeled receptor subunits f_G can be obtained by using them as fit parameters in a least squares fit of N_{g-spot}, N_{r-spot}, and N_{y-spot} to the observed spot counts.

Supplementary Note 2

Model to calculate fluorescent GFP and labeled SNAP-tag fractions

The fractions of fluorescent GFP p_g and labeled SNAP-tags p_r can be obtained from the dually labeled SNAP549-PDGFRTM-GFP by counting the numbers N_{g-spot}, N_{r-spot}, and N_{y-spot} of green, red and yellow labeled spots. The coincidental overlap of red and green receptors to form a yellow spot needs to be considered. The formulas from Suppl. Note 1 can be simplified because there are only receptors carrying both a GFP ad a SNAP-tag.

With the molecule number N_0, p_g and, p_r we directly get:

$$N_y = N_0 \cdot p_g \cdot p_r$$

$$N_g = N_0 \cdot p_g \cdot (1 - p_r)$$

$$N_r = N_0 \cdot \left(1 - p_g\right) \cdot p_r$$

The rest of the equations remains as in Suppl. Note 1:

$$p_{rand} = 1 - (1 - A_s/A_0)^{N_r}$$

$$N_{y-rand} = N_g \cdot (1 - (1 - A_s/A_0)^{N_r})$$

$$N_{g-spot} = N_g - N_{y-rand}$$

$$N_{r-spot} = N_r - N_{y-rand}$$

$$N_{y-spot} = N_y + N_{y-rand}$$

Estimates for the total number of receptor subunits N_0, the fraction of fluorescent GFP p_g, and the fraction of labeled SNAP-tags p_r can be obtained by using them as fit parameters in a least squares fit of N_{g-spot}, N_{r-spot}, and N_{y-spot} to the observed spot counts.

Supplementary Note 3

Fraction of receptor subunits in dimers in dependence on total subunit density

The fraction f_d of receptor subunits in dimers is

$$f_d = \frac{2[D]}{2[D]+[M]},$$

where $[M]$ and $[D]$ are the concentrations of monomers and dimers. The dissociation constant k_d is given by

$$k_d = \frac{[M]^2}{[D]}$$

and the receptor subunit density $[R]$ is

$$[R] = 2[D] + [M].$$

Combining the three equations to eliminate $[M]$ and $[D]$ yields the quadratic equation

$${f_d}^2 + (-2 - k_d/2[R])\, f_d + 1 = 0,$$

which has only one solution satisfying $0 \leq f_d \leq 1$, which is

$$f_d = 1 + \left(k_d - \sqrt{k_d(k_d + 8[R])}\right)/4[R].$$